Inorg. Chem. **2007**, *46*, 9254–9261

Spectroelectrochemistry and DFT Analysis of a New $\{RuNO\}^n$ Redox System with Multifrequency EPR Suggesting Conformational Isomerism in the $\{RuNO\}^7$ State

Priti Singh,[†] Jan Fiedler,[‡] Stanislav Záliš,[‡] Carole Duboc,[§] Mark Niemeyer,[†] Falk Lissner,[†] Thomas Schleid,[†] and Wolfgang Kaim[†,*]

Institut für Anorganische Chemie, Universität Stuttgart, Pfaffenwaldring 55, D-70550 Stuttgart, Germany, J. Heyrovský Institute of Physical Chemistry, v.v.i., Academy of Sciences of the Czech Republic, Dolejškova 3, CZ-18223 Prague, Czech Republic, Grenoble High Magnetic Field Laboratory, Laboratoire des Champs Magnétiques Intenses CNRS, 25, Avenue des Martyrs, BP 166, F-38042 Grenoble Cedex 9, France

Received June 20, 2007

The compound $[Ru(NO)(bpym)(terpy)](PF_6)_3$, bpym = 2,2′-bipyrimidine and terpy = 2,2′:6′,2″-terpyridine, with a $\{RuNO\}^6$ configuration (angle Ru–N–O 175.2(4)°) was obtained from the structurally characterized precursor $[Ru(NO_2)(bpym)(terpy)](PF_6)$, which shows bpym-centered reduction and metal-centered oxidation, as evident from EPR spectroscopy. The relatively labile $[Ru(NO)(bpym)(terpy)]^{3+}$, which forms a structurally characterized acetonitrile substitution product $[Ru(CH_3CN)(bpym)(terpy)](PF_6)_2$ upon treatment with CH_3OH/CH_3CN, is electrochemically reduced in three one-electron steps of which the third, leading to neutral [Ru(NO)(bpym)(terpy)], involves electrode adsorption. The first-two reduction processes cause shifts of ν(NO) from 1957 via 1665 to 1388 cm^{-1}, implying a predominantly NO-centered electron addition. UV–vis-NIR Spectroscopy shows long-wavelength ligand-to-ligand charge transfer absorptions for $[Ru^{II}(NO^{-I})(bpym)(terpy)]^+$ in the visible region, whereas the paramagnetic intermediate $[Ru(NO)(bpym)(terpy)]^{2+}$ exhibits no distinct absorption maximum above 309 nm. EPR spectroscopy of the latter at 9.5, 95, and 190 GHz shows the typical invariant pattern of the $\{RuNO\}^7$ configuration; however, the high-frequency measurements at 4 and 10 K reveal a splitting of the g_1 and g_2 components, which is tentatively attributed to conformers resulting from the bending of RuNO. DFT calculations support the assignments of oxidation states and the general interpretation of the electronic structure.

Introduction

After the discovery of the variegated physiological roles[1] of NO, the coordination chemistry[2] of this non-innocent[3] ligand with its possible NO^+, $NO^•$,[4] NO^-,[5] and potentially even more-negative[6] oxidation states has experienced a revival,[2,7] especially in connection with iron as the natural metal-binding center. However, the complexes of the NO redox system with the heavier homologue ruthenium have also attracted interest,[8] for example from medical-pharma-

* To whom correspondence should be addressed. E-mail: kaim@iac.uni-stuttgart.de.
† Universität Stuttgart.
‡ J. Heyrovský Institute of Physical Chemistry, v.v.i.
§ Grenoble High Magnetic Field Laboratory.

(1) (a) Murad, F. *Angew. Chem., Int. Ed.* **1999**, *28*, 1856. (b) Wang, P. G.; Xian, M.; Tang, X.; Wu, X.; Wen, Z.; Cai, T.; Janczuk, A. *Chem. Rev.* **2002**, *102*, 1091. (c) Hrabie, J. A.; Keefer, L. K. *Chem. Rev.* **2002**, *102*, 1135.
(2) (a) McCleverty, J. A. *Chem. Rev.* **2004**, *104*, 403. (b) Enemark, J. H.; Feltham, R. D. *Coord. Chem. Rev.* **1974**, *13*, 339. (c) Westcott, B. L.; Enemark, J. L. In *Inorganic Electronic Structure and Spectroscopy*; Solomon, E. I., Lever, A. B. P., Eds.; Wiley & Sons: New York, 1999; Vol. 2, p 403.
(3) (a) Jørgensen, C. K. *Oxidation Numbers and Oxidation States*; Springer Publishing: Berlin, 1969. (b) Ward, M. D.; McCleverty, J. A. *J. Chem. Soc., Dalton Trans.* **2002**, 275.
(4) Wanner, M. M.; Scheiring, T.; Kaim, W.; Slep, L. D.; Baraldo, L. M.; Olabe, J. A.; Zalis, S.; Baerends, E. J. *Inorg. Chem.* **2001**, *40*, 5704.
(5) (a) Wanat, A.; Schneppensieper, T.; Stochel, G.; van Eldik, R.; Bill, E.; Wieghardt, K. *Inorg. Chem.* **2002**, *41*, 4. (b) Ghosh, P.; Stobie, K.; Bill E.; Bothe, E.; Weyhermüller, T.; Ward, M. D.; McCleverty, J. A.; Wieghardt, K. *Inorg. Chem.* **2007**, *46*, 522.
(6) Landry, V. K.; Pang, K.; Quan, S. M.; Parkin, G. *Dalton Trans.* **2007**, 820.
(7) (a) *Nitric Oxide Donors*; Wang, P. G., Cai, T. B., Taniguchi, N. Eds.; Wiley-VCH: Weinheim, Germany, 2005. (b) *Activation of Small Molecules*; Tolman, W. B. Ed.; Wiley-VCH: Weinheim, Germany, 2006; p 43.

10.1021/ic701206a CCC: $37.00
Published on Web 09/28/2007

ceutical,[9] catalysis, molecular electronics, or photochemical viewpoints.[10] Also, the considerably covalent metal−ligand bonding as expressed by the Enemark−Feltham[2b] notation {MNO}^{n} has been well vindicated by the almost-invariant X-band (9.5 GHz) EPR characteristics (g factors, A(^{14}N)) of a number of {RuNO}^{7} species with very diverse ligand configurations.[11] Confirmation and additional information for these X-band EPR results was now sought with the help of high-field EPR, here W-band (95 GHz) and G-band (190 GHz) EPR. The requirement for such a study, a {RuNO}^{7} complex with sufficient chemical stability in high concentration, was found in the one-electron reduced form of the new [Ru(NO)(bpym)(terpy)](PF$_6$)$_3$, bpym = 2,2′-bipyrimidine and terpy = 2,2′:6′,2″-terpyridine, which was obtained from the X-ray structurally characterized precursor [Ru(NO$_2$)(bpym)(terpy)](PF$_6$). These mononuclear compounds related to an isomeric analogue involving 2,2′-bipyrazine[11] are also required for the ongoing attempts to prepare conjugatively bridged dinuclear complexes such as {(μ-bpym)[Ru(NO)(terpy)]$_2$}$^{n+}$.

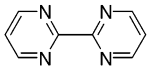

2,2'-bipyrimidine (bpym)

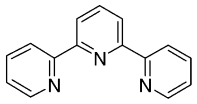

2,2':6',2"-terpyridine (terpy)

The redox system [Ru(NO)(bpym)(terpy)]$^{3+/2+/+/o}$ has been studied by cyclic voltammetry and, except for the final member of the series, by spectroelectrochemistry in the UV−vis-NIR and IR (ν(NO)) regions. These studies were undertaken because the presence of three different π acceptors (NO$^+$, bpym, terpy) as ligands to π-electron-donating ruthenium(II) raises various possibilities for electron- and charge-transfer processes; the sequence of low-lying π* levels was to be established through the combination of spectroscopic methods and through DFT calculations.

Experimental Section

Instrumentation. EPR spectra in the X band were recorded with a Bruker System EMX. EPR spectra at 95 and 190 GHz were recorded using a multifrequency spectrometer.[12] A Gunn diode operating at 95 GHz and equipped with a second harmonic generator has been used as a radiation source. An InSb bolometer (QMC Instruments) was used for detection. The main magnetic field was provided by a superconducting magnet (Cryogenics Consultant), which generates fields of up to 12 T. Owing to different field-sweep conditions, the absolute values of the g components were obtained by calibrating the precisely measured g anisotropy data with the isotropic g value from X-band measurements. Whereas this procedure does not account for the temperature dependence of g, the values extracted are identical with those obtained using an added standard. The accuracy of g values is estimated at ±0.0003. ^{1}H NMR spectra were taken on a Bruker AC 400 spectrometer. IR spectra were obtained using a Nicolet 6700 FTIR instrument; solid-state IR measurements were performed with an ATR unit (smart orbit with diamond crystal). UV−vis-NIR absorption spectra were recorded on J&M TIDAS and Shimadzu UV 3101 PC spectrophotometers. Cyclic voltammetry was carried out in 0.1 M Bu$_4$NPF$_6$ solutions using a three-electrode configuration (glassy-carbon working electrode, platinum counter electrode, Ag/AgCl reference) and a PAR 273 potentiostat and function generator. The ferrocene/ferrocenium (Fc/Fc$^+$) couple served as an internal reference. Polarography was performed using a PAR 263A instrument. Spectroelectrochemistry was performed using an optically transparent thin-layer electrode (OTTLE) cell.[13] A two-electrode capillary served to generate intermediates for X-band EPR studies.[14]

Syntheses. [Ru(NO$_2$)(bpym)(terpy)](PF$_6$). An amount of 100 mg (0.227 mmol) Ru(terpy)Cl$_3$[15] and 107 mg (0.681 mmol) bpym were heated to reflux for 4 h in a 50 mL ethanol/water (1:1, v/v) mixture under an argon atmosphere. An amount of 300 mg (4.347 mmol) NaNO$_2$ was added to the reddish-brown solution, and refluxing was continued for 3 h. After cooling, the dark-red solution was filtered, and a concentrated solution of NH$_4$PF$_6$ (5 mL) was added to the filtrate. The reddish-brown precipitate was filtered off, and the filtrate (mother liquor) was kept for slow crystallization. After 1 day, red-shiny crystals had grown in the solution, which were analytically pure. The solid obtained by the first filtration was recrystallized from a mixture of acetonitrile and diethylether (1:3) to get more analytically pure compound. Single crystals were grown by slow diffusion of diethylether into an acetonitrile solution at room temperature. Yield: 120 mg (0.176 mmol, 77%). Calcd for C$_{23}$H$_{17}$F$_6$N$_8$O$_2$PRu (683.48 g/mol): C, 40.42; H, 2.51; N: 16.39. Found: C, 40.27; H, 2.32; N, 16.19%. ^{1}H NMR (acetone-d_6): δ = 7.37 (dd, 1H), 7.43 (m, 2H), 8.08 (m, 5H), 8.24 (dd, 1H, J = 4.73 and 5.79 Hz), 8.36 (t, 1H, 8.08 Hz), 8.62 (dd, 2H), 8.76 (d, 2H, 8.08 Hz), 8.94 (dd, 1H, J = 4.73 and 2.05 Hz), 9.38 (dd, 1H, J = 4.73 and 2.03 Hz), 10.39 (dd, 1H, J = 5.95 and 2.13 Hz). ^{1}H NMR (CD$_3$CN): δ = 7.09 (dd, 1H, bpym, J = 5.64 and 4.70 Hz), 7.24 (m, 2H, terpy), 7.60 (dd, 1H, bpym, 5.50 and 2.05 Hz), 7.76 (m, 2H, terpy), 7.88 (dt, 2H, terpy, J(3) = 7.63 and J(2) =1.45 Hz), 7.97 (dd, 1H, bpym, J = 4.73 and 5.56 Hz), 8.15 (t, 1H, 8.16 Hz, terpy), 8.28 (m, 2H, terpy), 8.40 (d, 2H, 8.16 Hz, terpy), 8.76 (dd, 1H, bpym, J = 4.42 and 2.05 Hz), 9.20 (dd, 1H, bpym, J = 4.50 and 2.13 Hz), 10.16 (dd, 1H, bpym, J = 5.64 and 2.13 Hz). IR (KBr): 1342 (ν_{NO_2asym}) and 1286 cm^{-1} (ν_{NO_2sym}). UV/vis (CH$_3$CN): λ_{max}/nm (ϵ/M^{-1} cm^{-1}) = 238 (26 900), 264 (23 280), 308 (25 600), 330 (13 500, sh) 362 (6100), 470 (6500).

[Ru(NO)(bpym)(terpy)](PF$_6$)$_3$. HCl (10 mL at 3M) was added slowly to 100 mg of [Ru(bpym)(terpy)NO$_2$](PF$_6$)with constant stirring, which continued for 15 min. The deep-red color of the

(8) (a) Sarkar, S.; Sarkar, B.; Chanda, N.; Kar, S.; Mobin, S. M.; Fiedler, J.; Kaim, W.; Lahiri, G. K. *Inorg. Chem.* **2005**, *44*, 6092. (b) Videla, M.; Jacinto, J. S.; Baggio, R.; Garland, M. T.; Singh, P.; Kaim, W.; Slep, L. D.; Olabe, J. A. *Inorg. Chem.* **2006**, *45*, 8608. (c) Tfouni, E.; Queiroz Ferreira, K.; Gorzoni Doro, F.; Santana da Silva, R.; Novais da Rocha, Z. *Coord. Chem. Rev.* **2005**, *249*, 405. (d) Maji, S.; Chatterjee, C.; Mobin, S. M.; Lahiri, G. K. *Eur. J. Inorg. Chem.* **2007**, 3425. (e) Chen, Y.; Lin, F.-T.; Shepherd, R. E. *Inorg. Chem.* **1999**, *38*, 973.

(9) (a) Karidi, K.; Garoufis, A.; Hadjiliadis, N.; Lutz, M.; Spek, A. L.; Reedijk, J. *Inorg. Chem.* **2006**, *45*, 10282. (b) Serli, B.; Zangrando, E.; Gianferrara, T.; Yellowlees, L.; Alessio, E. *Coord. Chem. Rev.* **2003**, *245*, 73. (c) Tfouni, E.; Krieger, M.; McGarvey, B. R.; Franco, D. W. *Coord. Chem. Rev.* **2003**, *236*, 57. (d) Patra, A. K.; Mascharak, P. K. *Inorg. Chem.* **2003**, *42*, 7363.

(10) Ford, P. S.; Laverman, L. E. *Coord. Chem. Rev.* **2005**, *249*, 391.

(11) Frantz, S.; Sarkar, B.; Sieger, M.; Kaim, W.; Roncaroli, F.; Olabe, J. A.; Zalis, S. *Eur. J. Inorg. Chem.* **2004**, 2902.

(12) Barra, A.-L.; Brunel, L.-C.; Robert, J. B. *Chem. Phys. Lett.* **1990**, *165*, 107. (b) Muller, F.; Hopkins, M. A.; Coron, N.; Gryndberg, M.; Brunel, L.-C.; Martinez, G. *Rev. Sci. Instrum.* **1989**, *60*, 3681.

(13) Krejcik, M.; Danek, M.; Hartl, F. *J. Electroanal. Chem.* **1991**, *317*, 179.

(14) Kaim, W.; Ernst, S.; Kasack, V. *J. Am. Chem. Soc.* **1990**, *112*, 173.

(15) Sullivan, B. P.; Calvert, J. M.; Meyer, T. J. *Inorg. Chem* **1990**, *19*, 1404.

Table 1. Selected Crystallographic Data for Complexes $[Ru(NO_2)(bpym)(terpy)](PF_6)$, $[Ru(NO)(bpym)(terpy)](PF_6)_3$ and $[Ru(CH_3CN)(bpym)(terpy)](PF_6)_2$[a]

formula	$C_{23}H_{17}F_6N_8O_2PRu$	$C_{23}H_{17}F_{18}N_8OP_3Ru$	$C_{25}H_{20}F_{12}N_8P_2Ru$
fw	683.49	957.43	823.50
color, habit	red, needle	yellow, rod	red, needle
cryst size (mm^3)	$0.65 \times 0.12 \times 0.06$	$0.3 \times 0.05 \times 0.05$	$0.50 \times 0.12 \times 0.12$
cryst syst	monoclinic	orthorhombic	monoclinic
space group	$P2_1/n$	*Pbca*	$P2_1/n$
a (Å)	8.9165(17)	14.7169(2)	10.532(2)
b (Å)	15.8829(19)	17.8342(2)	12.828(3)
c (Å)	19.321(3)	23.8615(2)	23.516(5)
β (deg)	95.216(15)	90.00	94.148(13)
V ($Å^3$)	2724.9(7)	6262.79(12)	3168.7(12)
Z	4	8	4
d_{calcd} (g/cm^3)	1.666	2.031	1.726
μ (mm^{-1})	0.713	0.800	0.699
T (K)	173	100	173
2θ range (deg)	3−52	7−57	3−54
collected data	5651	57 209	7278
unique data/R_{int}	5303/0.056	7661/0.177	6905/0.053
data with $I > 2\sigma(I)$ (N_o)	2898	5474	3364
no. of params (N_p)	371	487	434
$R1$ ($I > 2\sigma(I)$)[b]	0.0534	0.0868	0.0763
$WR2$ (all data)[c]	0.1316	0.1367	0.2232
GOF[d]	0.827	1.189	1.003
resd dens ($e/Å^3$)	0.98/−1.17	0.87/−1.11	0.95/−0.72

[a] All of the data were collected using Mo Kα ($\lambda = 0.71073$ Å) radiation. [b] $R1 = \sum(||F_o| - |F_c||)/\sum(|F_o|$. [c] $wR2 = \{\sum[w(F_o^2 - F_c^2)^2]/\sum[w(F_o^2)^2]\}^{1/2}$. [d] GOF $= \{\sum[w(F_o^2 - F_c^2)^2]/(N_o - N_p)\}^{1/2}$.

solution changed to yellow-brown. A saturated solution of NH_4PF_6 (10 mL) was added to the mixture, and 10 mL of more water was added to complete the precipitation. A light-yellow solid was filtered from the orange solution and washed with ice-cold water. The analytically pure compound was obtained by dissolving the solid in a minimum volume of CH_3CN, followed by precipitation with diethylether. Single crystals were grown by slow diffusion of dichloromethane into an acetonitrile solution at room temperature. Yield: 134 mg (0.140 mmol, 96%). Calcd for $C_{23}H_{17}F_{18}N_8OP_3Ru$ (957.42 g/mol): C, 28.85; H, 1.79; N, 11.70. Found: C, 28.82; H, 1.83; N, 11.79%. ^{1}H NMR (acetone-d_6): $\delta = 7.80$ (dd, 1H, $J =$ 4.80 and 6.02 Hz), 7.85 (m, 2H), 8.22 (dd, 1H, $J = 4.73$ and 5.79 Hz), 8.60 (m, 5H), 9.02 (d, 2H, 8.08 Hz), 9.19 (m, 3H), 9.39 (dd, 1H, $J = 4.50$ and 1.83 Hz), 9.79 (dd, 1H, $J = 4.73$ and 2.03 Hz), 10.32 (dd, 1H, $J = 5.72$ and 1.90 Hz). ^{1}H NMR (CD_3CN): $\delta =$ 7.54 (dd, 1H, bpym, $J = 5.87$ and 1.90 Hz), 7.69 (dd, 1H, bpym, 5.64 and 4.80 Hz), 7.76(m, 2H, terpy), 8.16 (m, 2H, terpy), 8.42-(dd, 1H, bpym, $J = 4.80$ and 5.57 Hz), 8.50 (dt, 2H, terpy, J(3) = 7.93 and J(2) = 1.44 Hz), 8.73 (m, 2H, terpy), 8.88 (d, 2H, 7.78 Hz, terpy), 9.00 (t, 1H, 7.78 Hz, terpy), 9.30 (dd, 1H, bpym, $J =$ 4.65 and 1.90 Hz), 9.66 (dd, 1H, bpym, $J = 5.72$ and 1.90 Hz), 9.71 (dd, 1H, bpym, $J = 4.80$ and 1.90 Hz). IR (KBr): $\nu_{NO} =$ 1957 cm^{-1}, $\nu_{PF_6} = 835$ cm^{-1}, $\nu_{Ru-N-O} = 558$ cm^{-1}.

$[Ru(CH_3CN)(bpym)(terpy)](PF_6)_2$. Attempts to recrystallize $[Ru(NO)(bpym)(terpy)](PF_6)_3$ in methanol/acetonitrile (1:1, v/v) mixture gave crystals of $[Ru(CH_3CN)(bpym)(terpy)](PF_6)_2$, which were analyzed by single-crystal X-ray crystallography and ^{1}H NMR. ^{1}H NMR (CD_3CN): δ/ppm = 7.23 (dd, 1H, bpym, $J = 5.79$ and 6.02 Hz), 7.40(m, 2H, terpy), 7.64 (dd, 1H, bpym, 5.72 and 2.05 Hz), 7.83(m, 2H, terpy), 8.06 (dt, 2H, terpy, J(3) = 7.86 and J(2) = 1.53 Hz), 8.10(dd, 1H, bpym, $J = 6.02$ and 4.82 Hz), 8.37 (t, 1H, terpy, 8.10 Hz), 8.45 (m, 2H, terpy), 8.59 (d, 2H, terpy, 8.15 Hz,), 8.87 (dd, 1H, bpym, $J = 4.73$ and 2.04 Hz), 9.40 (dd, 1H, bpym, $J = 4.73$ and 2.04 Hz), 9.85 (dd, 1H, bpym, $J = 5.72$ and 2.05 Hz).

Crystallography. X-ray quality crystals of $[Ru(NO_2)(bpym)(terpy)](PF_6)$, $[Ru(NO)(bpym)(terpy)](PF_6)_3$, and $[Ru(CH_3CN)(bpym)(terpy)](PF_6)_2$ were obtained as described above. Suitable crystals were selected under a cover of viscous hydrocarbon oil (Paratone N, Exxon), attached to a glass fiber, and instantly placed in a low-temperature N_2-stream.[16a] The data were collected at low temperatures using a Siemens P4 diffractometer (nitro and acetonitrile complexes, 173 K) or Kappa CCD (Nonius, 100 K; nitrosyl complex). Crystal data are given in Table 1. Calculations were performed with the *SHELXTL* PC 5.03[16b] and *SHELXL-97*[16c] program systems installed on a local PC. The structures were solved by direct methods and refined on F_o^2 by full-matrix least-squares refinement. Absorption corrections were applied using semiempirical ψ-scans (nitro and acetonitrile complexes) or applying the program *HABITUS*[16d] (numerical procedure) for the nitrosyl complex. Anisotropic thermal parameters were included for all non-hydrogen atoms. Final R values are listed in Table 1, and important bond parameters are provided in Tables 2 and S1. Further details are given in the Supporting Information.

DFT Calculations. The electronic structures of $[Ru(NO)(bpym)(terpy)]^{n+}$ ($n = 1-3$) and $[Ru(NO_2)(bpym)(terpy)]^+$ were calculated by density functional theory (DFT) methods using the *Gaussian 03*[17] and *ADF2006.01*[18] program packages. The calculations of the vibrational frequencies were performed at optimized geometries.

For the hydrogen, carbon, nitrogen, and oxygen atoms, 6-31G* polarized double-ζ basis sets[19] (G03) were used together with quasirelativistic effective core pseudopotentials and a corresponding optimized set of basis functions for ruthenium.[20] The vibrational analysis was done with the pure density functional BPW91.[21,22]

Slater-type orbital basis sets of triple-ζ quality with two polarization functions for the ruthenium atom and of triple-ζ quality with one polarization function for the remaining atoms were employed within *ADF2006.01*. The inner shells were represented by the frozen core approximation (1s for C, N, O, 1s-3d for ruthenium were kept frozen). The calculations were done with the functional including Becke's gradient correction[21] to the local

(16) (a) Hope, H. *Progr. Inorg. Chem.* **1995**, *41*, 1. (b) *SHELXTL*, PC 5.03; Siemens Analytical X-Ray Instruments Inc.: Madison, WI, 1994. (c) Sheldrick, G. M. *Program for Crystal Structure Solution and Refinement*, Universität Göttingen: Göttingen, Germany, 1997. (d) Herrendorf, W.; Bärnighausen, H. *HABITUS*; Karlsruhe, Germany, 1993.

Table 2. Comparison of Selected Bond Lengths (Angstroms) and Angles (Degrees) of Complexes with ADf/BP Calculation Results

	$[Ru(NO_2)(bpym)(terpy)](PF_6)$		$[Ru(NO)(bpym)(terpy)](PF_6)_3$	
	exptl	calcd	exptl	calcd
Ru−N1	2.034(5)	2.055	1.770(5)	1.775
Ru−N2	1.975(5)	1.967	1.992(5)	2.012
Ru−N3	2.079(5)	2.089	2.069(5)	2.121
Ru−N4	2.068(5)	2.075	2.088(5)	2.121
Ru−N5	2.070(5)	2.099	2.088(5)	2.126
Ru−N6	2.090(5)	2.119	2.093(5)	2.136
N1−O1	1.264(6)	1.253	1.129(6) (N1−O)	1.143
N1−O2	1.246(6)	1.240		
N1−Ru−N5	174.8(2)	172.1	172.1(2)	172.0
N2−Ru−N6	172.50(19)	176.3	168.59(18)	169.6
N3−Ru−N4	159.01(19)	158.1	159.40(19)	157.2
N1−Ru−N2	90.18(19)	88.4	96.7(2)	95.7
N1−Ru−N3	91.8(2)	88.6	92.3(2)	93.9
N1−Ru−N4	87.0(2)	88.4	95.4(2)	94.0
N1−Ru−N6	96.8(2)	95.3	94.6(2)	94.7
N2−Ru−N3	80.4(2)	79.4	80.20(19)	79.0
N2−Ru−N4	78.7(2)	78.8	79.95(19)	79.0
N2−Ru−N5	94.93(19)	99.5	91.03(19)	92.3
N3−Ru−N5	88.41(19)	92.2	87.02(18)	87.6
N4−Ru−N5	94.7(2)	93.7	87.88(18)	87.5
N4−Ru−N6	104.2(2)	100.6	100.91(18)	100.3
N5−Ru−N6	78.0(2)	76.8	77.66(18)	77.3
O−N1−Ru			175.2(4)	177.4
O1−N1−O2	118.6(5)	121.7		

exchange expression in conjunction with Perdew's gradient correction[23] to the local correlation (ADF/BP). The scalar relativistic zero-order regular approximation (ZORA) was used within ADF calculations. The *g* tensor was obtained from a spin-nonpolarized wave function after incorporating the spin−orbit coupling. *A* and *g* tensors were obtained by first-order perturbation theory from a ZORA Hamiltonian in the presence of a time-independent magnetic field.[24]

Results and Discussion

Synthesis. The complex salt $[Ru(NO)(bpym)(terpy)](PF_6)_3$ was obtained from the nitro precursor compound $[Ru(NO_2)(bpym)(terpy)](PF_6)$ in analogy to previously reported procedures for related nitrosylruthenium complexes.[8,11] Spectroscopic properties of the precursor are given in the Experimental Section, the molecular structure and electrochemistry will be discussed below. The use of potentially bis-bidentate 2,2′-bipyrimidine as opposed to, e.g., 2,2′-bipyridine or 2,2′-bipyrazine[11] was aimed at obtaining dinuclear complexes $\{(\mu\text{-bpym})[Ru(NO)(terpy)]_2\}^{n+}$.

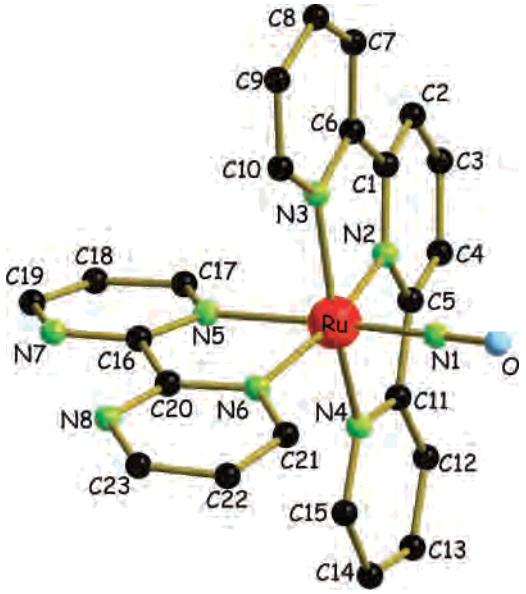

Figure 1. Molecular structure of the trication of $[Ru(NO)(bpym)(terpy)](PF_6)_3$ in the crystal.

Crystal Structures. The precursor compound $[Ru(NO_2)(bpym)(terpy)](PF_6)$ could be crystallized to exhibit a typical[8a,25] nitro complex structure (Tables 1, 2, and Figure S1 of the Supporting Information). The meridional binding of terpy[26] causes one metal-bound nitrogen of coordinated bpym to lie in the cis position and another one to lie in the trans position to NO_2^-. The polar axis of terpy lies approximately in the O_2NRu plane. The bond parameters are not unusual and will not be discussed further.

The molecular structure of the trication in the crystal (Table 1) of $[Ru(NO)(bpym)(terpy)](PF_6)_3$ confirms the $\{RuNO\}^6$ state via the nearly linear (175.2(4)°) RuNO configuration (Figure 1, Table 2) and the typical[8] Ru−N (1.770(5)) and N−O (1.129(6) Å) bond lengths. Recrystallizing this material from $MeOH/CH_3CN$ showed the lability of the ruthenium-nitrosyl bond as a result of the cumulation of three acceptor ligands at Ru^{II} and high positive charge, producing structurally characterized $[Ru(CH_3CN)(bpym)(terpy)](PF_6)_2$ (Tables 1 and S1, Figure S2 in the Supporting Information). Table 2 confirms that the DFT-optimized geometries of $[Ru(NO)(bpym)(terpy)]^{3+}$ and $[Ru(NO_2)(bpym)(terpy)]^+$ agree with the experimental structural data. The Ru−N1 and Ru−N2 bond lengths are reproduced within 0.02 Å, and the remaining Ru−N bond lengths are slightly

(17) Frisch, M. J.; Trucks, G. W.; Schlegel, H. B.; Scuseria, G. E.; Robb, M. A.; Cheeseman, J. R.; Montgomery, J. A., Jr.; Vreven, T.; Kudin, K. N.; Burant, J. C.; Millam, J. M.; Iyengar, S. S.; Tomasi, J.; Barone, V.; Mennucci, B.; Cossi, M.; Scalmani, G.; Rega, N.; Petersson, G. A.; Nakatsuji, H.; Hada, M.; Ehara, M.; Toyota, K.; Fukuda, R.; Hasegawa, J.; Ishida, M.; Nakajima, T.; Honda, Y.; Kitao, O.; Nakai, H.; Klene, M.; Li, X.; Knox, J. E.; Hratchian, H. P.; Cross, J. B.; Bakken, V.; Adamo, C.; Jaramillo, J.; Gomperts, R.; Stratmann, R. E.; Yazyev, O.; Austin, A. J.; Cammi, R.; Pomelli, C.; Ochterski, J. W.; Ayala, P. Y.; Morokuma, K.; Voth, G. A.; Salvador, P.; Dannenberg, J. J.; Zakrzewski, V. G.; Dapprich, S.; Daniels, A. D.; Strain, M. C.; Farkas, O.; Malick, D. K.; Rabuck, A. D.; Raghavachari, K.; Foresman, J. B.; Ortiz, J. V.; Cui, Q.; Baboul, A. G.; Clifford, S.; Cioslowski, J.; Stefanov, B. B.; Liu, G.; Liashenko, A.; Piskorz, P.; Komaromi, I.; Martin, R. L.; Fox, D. J.; Keith, T.; Al-Laham, M. A.; Peng, C. Y.; Nanayakkara, A.; Challacombe, M.; Gill, P. M. W.; Johnson, B.; Chen, W.; Wong, M. W.; Gonzalez, C.; Pople, J. A. *Gaussian 03*, revision C.02; Gaussian, Inc.: Wallingford, CT, 2004.
(18) (a) te Velde, G.; Bickelhaupt, F. M.; van Gisbergen, S. J. A.; Fonseca Guerra, C.; Baerends, E. J.; Snijders, J. G.; Ziegler, T. *J. Comput. Chem.* **2001**, *22*, 931−967. (b) ADF2004.01, SCM, Theoretical Chemistry, Vrije Universiteit: Amsterdam, The Netherlands, http://www.scm.com.
(19) Hariharan, P. C.; Pople, J. A. *Theor. Chim. Acta* **1973**, *28*, 213.
(20) Andrae, D.; Häussermann, U.; Dolg, M.; Stoll, H.; Preuss, H. *Theor. Chim. Acta* **1990**, *77*, 123.
(21) Becke, A. D. *Phys. Rev. A* **1988**, *38*, 3098.
(22) Perdew, J. P.; Wang, Y. *Phys. Rev. B* **1992**, *45*, 13244.
(23) Perdew, J. P. *Phys. Rev. B* **1986**, *33*, 8822.
(24) (a) van Lenthe, E.; van der Avoird, A.; Wormer, P. E. S. *J. Chem. Phys.*, **1997**, *107*, 2488. (b) van Lenthe, E.; van der Avoird, A.; Wormer, P. E. S. *J. Chem. Phys.*, **1998**, *108*, 4783.
(25) Hitchman, M. A.; Rowbottom, G. L. *Coord. Chem. Rev.* **1982**, *42*, 55.
(26) Schubert, U.; Hofmeier, H.; Newkome, G. R. *Modern Terpyridine Chemistry*; Wiley-VCH: Weinheim, Germany, 2006.

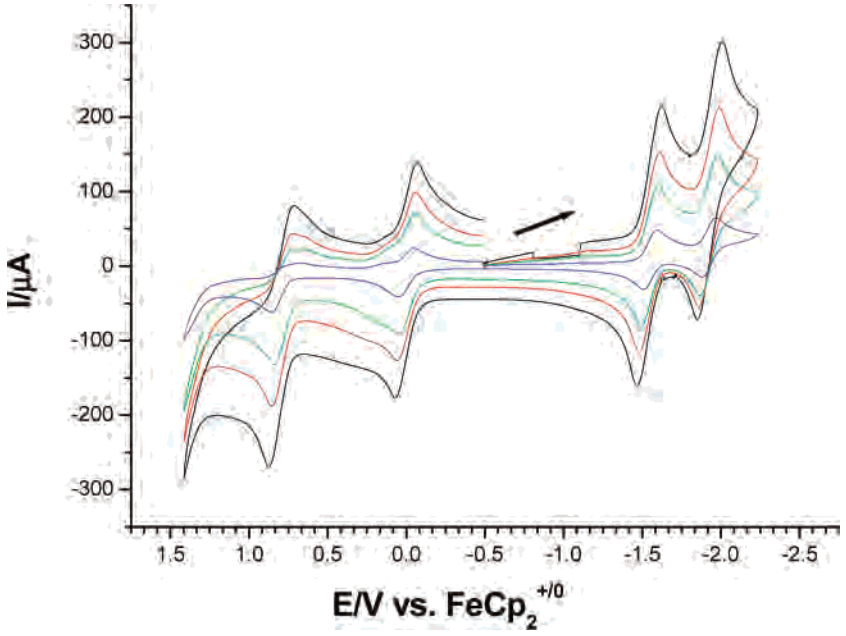

Figure 2. Cyclic voltammograms of $[Ru(NO_2)(bpym)(terpy)](PF_6)$ (1 mM) in CH_3CN/0.1 M Bu_4NPF_6 at 298 K at variable scan rates (100, 500, 1000, 2000 mV/s); second peak from left: ferrocene standard.

overestimated. ADF/BP calculations give a slightly better description of the bonding parameters than the G03/B3LYP approach.

Electrochemistry. Cyclic voltammetry and polarography were employed to study the nitro precursor and electron-deficient $[Ru(NO)(bpym)(terpy)](PF_6)_3$. The nitro complex $[Ru(NO_2)(bpym)(terpy)](PF_6)$ exhibits a conventional electrochemical pattern (Figure 2) with one metal-centered oxidation (the Ru^{III} form slowly disintegrates) and two ligand-centered reductions, the first reduction identified with the formation of a ruthenium(II)-bonded bpym radical anion.[14] This interpretation is not only in agreement with the redox potentials[27] but also with EPR results for electrogenerated species (cf. below).

The very positive first reduction potential of +0.17 V versus $Fc^{+/o}$ of $[Ru(NO)(bpym)(terpy)](PF_6)_3$ in CH_3CN/0.1 M Bu_4NPF_6 facilitated the generation of the intermediate $[Ru(NO)(bpym)(terpy)]^{2+}$ with sufficient stability and concentration to carry out the high-field EPR investigations. After a second clean one-electron reversible reduction at −0.47 V, the third electron addition at −1.61 V evokes the appearance of a sharp desorption spike in the reverse scan of the cyclic voltammogram (Figure 3). Electrode adsorption of the reduction product results from the neutrality of the generated species $[Ru(NO)(bpym)(terpy)]^o$, which contains an extended π system in terpy; polarography confirmed the otherwise reversible one-electron transition at this step. Although not accessible by spectroelectrochemistry (cf. below), the potential of −1.61 V suggests reduction of Ru^{II}-coordinated 2,2′-bipyrimidine.[27]

The difference of 0.65 V between the potentials for first and second reduction is similar to that observed for other complexes involving the $NO^{+/\bullet/-}$ redox system;[8,11] however,

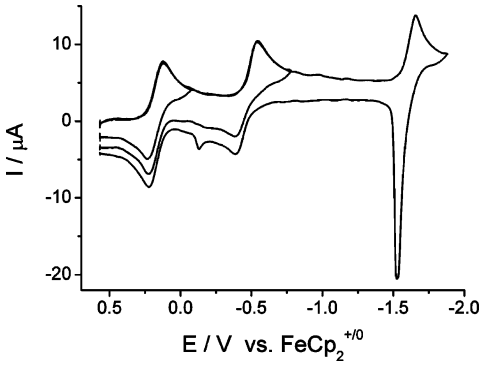

Figure 3. Cyclic voltammograms of $[Ru(NO)(bpym)(terpy)](PF_6)_3$ (1 mM) in CH_3CN/0.1 M Bu_4NPF_6 at 298 K at 200 mV/s.

spectroelectrochemistry was required to establish this assertion for NO being the target of the first-two electron additions.

IR Spectroelectrochemistry. Because of strong electrode adsorption during the third reduction step, the OTTLE spectroelectrochemical measurements in CD_3CN/0.1 M Bu_4NPF_6 could be carried out only for the charged species, that is, involving the first-two reduction processes. The ν(NO) stretching band has been long recognized as an excellent indicator for the oxidation state of that noninnocent ligand in metal complexes.[2,4,5,8,28] The starting form $[Ru(NO)(bpym)(terpy)]^{3+}$ exhibits a rather high value of 1957 cm^{-1} for ν(NO), which illustrates the π acceptor influence from both bpym and terpy just like the positive reduction potential.[8b] The shift of ν(NO) on one-electron reduction to 1665 cm^{-1} (Figure 4, top), that is, by 292 cm^{-1}, signifies a largely NO-centered electron addition to form a complex of $NO^{\bullet}$.[2,4,28] The second reversible one-electron reduction causes

(27) Ernst, S. D.; Kaim, W. *Inorg. Chem.* **1989**, *28*, 1520.

(28) (a) Sieger, M.; Sarkar, B.; Zalis, S.; Fiedler, J.; Escola, N.; Doctorovich, F.; Olabe, J. A.; Kaim, W. *Dalton Trans.* **2004**, 1797. (b) Singh, P.; Sarkar, B.; Sieger, M.; Niemeyer, M.; Fiedler, J.; Záliš, S.; Kaim, W. *Inorg. Chem.* **2006**, *45*, 4602.

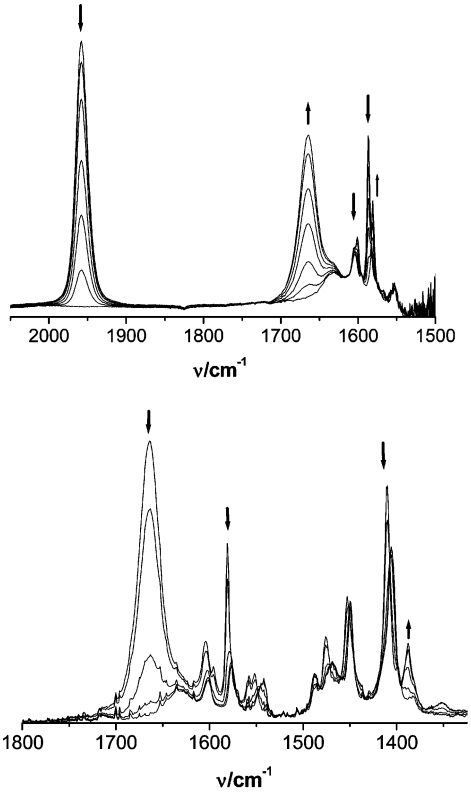

Figure 4. IR spectroelectrochemical response of [Ru(NO)(bpym)(terpy)]-$(PF_6)_3$ in CD_3CN/0.1 M Bu_4NPF_6 at 298 K: first (top) and second reduction step (bottom).

a similar shift of 277 cm^{-1} to produce a significant new feature, a band at 1388 cm^{-1} with diminished intensity (Figure 4, bottom), which would be a typical value for metal-coordinated NO^-.[5,6,8a,e]

From this experiment, we conclude that the first two reductions involve mainly the NO ligand, a result that is partially supported for the paramagnetic intermediate [Ru(NO)(bpym)(terpy)]$^{2+}$ by EPR spectroscopy.

Variable Frequency EPR Spectroscopy. EPR spectroscopy of both of the electrogenerated complexes, [Ru(NO_2)(bpym)(terpy)]$^{2+}$ (oxidative) and [Ru(NO_2)(bpym)(terpy)]^0 (reductive), indicated conventional electronic situations: The metal-centered oxidation leads to a ruthenium(III) species with $g_{1,2} = 2.365$ and $g_3 = 2.025$ (110 K, CH_3CN/0.1 M Bu_4NPF_6). Such values are typical for the low-spin $4d^5$ configuration of largely unperturbed Ru^{III}.[29,30] On the other hand, one-electron reduction produces a radical complex with a slight rhombic g anisotropy at $g_1 = 2.006$, $g_2 = 1.999$, $g_3 = 1.994$ (110 K), and with $g_{iso} = 1.995$ (298 K), a characteristic result for ruthenium(II) complexes of polypyridine radicals.[14] The stability of the intermediate [Ru(NO)(bpym)(terpy)]$^{2+}$ as obtained from reduction with zinc and the attainable high concentration in solution have allowed us to perform the first high-frequency EPR study of the nitrosylruthenium compound. High-field EPR studies of metal nitrosyl entities have been reported before for copper[31a] and iron[31b] systems. The conventional X-band measurements of [Ru(NO)(bpym)(terpy)]$^{2+}$ showed the typical invariant EPR characteristics[11] (g factors $g_1 > 2$, $g_2 \approx 2.0$, $g_3 < 2$; $A_2(^{14}N) \approx 3.4$ mT, Figure S3) of the {RuNO}^{7} species, which have been observed before for quite a number of different complexes containing that RuNO moiety.[11] In the present case, $g_1 = 2.021$, $g_2 = 1.995$, $g_3 = 1.885$, $A_2 = 3.4$ mT.

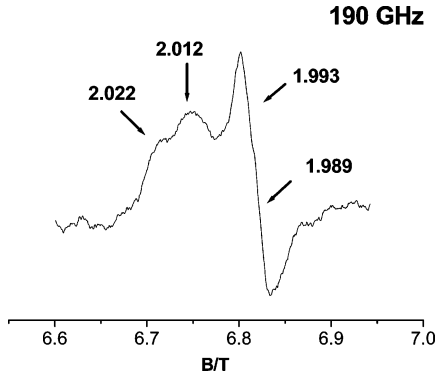

Figure 5. Central section (g_1, g_2) of the G-Band (190 GHz) EPR spectrum of [Ru(NO)(bpym)(terpy)]$^{2+}$ in CH_3CN at 4.2 K.

This result justifies once more the concept of rather-covalent metal−ligand bonding as expressed in the Enemark−Feltham notation {MNO}^{n}.[2b] Confirmation and additional information on these X-band EPR results was now sought with the help of high-frequency EPR, using W-band (95 GHz) and G-band (190 GHz) spectroscopy (Figures 5 and S4 in the Supporting Information).

The high-frequency EPR studies show the g factor components with better separation and unobstructed by hyperfine splitting. However, the 95 and especially the 190 GHz spectra also reveal two g_1 and two g_2 components (Figures 5 and S4 in the Supporting Information), suggesting the presence of two slightly different species. An explanation of this observation is based on the well-known bending of the {MNO}^{7} configuration,[2,7] which can lead to different conformers (staggered, eclipsed) as discussed previously for [M(NO$^•$)Cl_5] systems.[28] In the present situation with only one possible structure configuration (Figures 1 and S1 and S2 in the Supporting Information), the bending of RuNO can produce two different staggered conformations, having the RuNO plane between two neighboring pyridyl groups of terpy or between one terminal pyridine of terpy and the bpym plane and two possible eclipsed conformations. For [Os(NO)$Cl_5]^{n-}$, we have shown in a computational study that the g signature of different conformers can vary considerably;[28b] different such species characterized experimentally in matrices[32] have been associated with conformational isomerism.[28b]

Irrespective of the functional used, the DFT calculations indicate two energy minima, one eclipsed (RuNO plane almost coinciding with the RuN1N2 plane) and one staggered configuration (the RuNO plane between one terminal pyri-

(29) Patra, S.; Sarkar, B.; Mobin, S. M.; Kaim, W.; Lahiri, G. K. *Inorg. Chem.* **2003**, *42*, 6469.
(30) Poppe, J.; Moscherosch, M.; Kaim, W. *Inorg. Chem.* **1993**, *32*, 2640.
(31) (a) Pöppl, A.; Hartmann, M. *Stud. Surf. Sci. Catal.* **2002**, *142*, 375. (b) Yang, T. C.; Wolfe, M. D.; Neibergall, M. B.; Mekmouche, Y.; Lipscomb, J. D.; Hoffmann, B. M. *J. Am. Chem. Soc.* **2003**, *23*, 7056.
(32) (a) Eachus, R. S.; Baetzold, R. C.; Pawlik, Th. D.; Poluektov, O. G.; Schmidt, J. *Phys. Rev. B* **1999**, *59*, 8560. (b) Eachus, R. S.; Pawlik, Th. D.; Baetzold, R. C. *J. Phys.: Condens. Matter* **2000**, *12*, 8893.

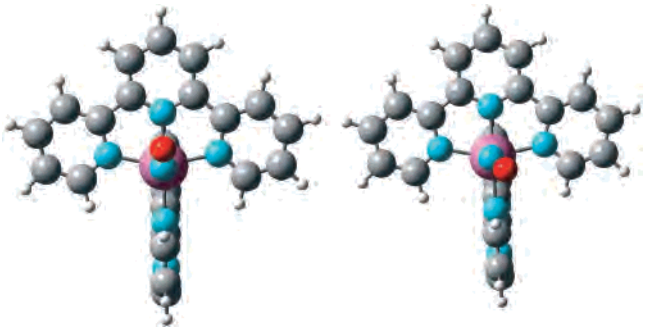

Figure 6. Different DFT-optimized conformations of [Ru(NO)(bpym)(terpy)]$^{2+}$ resulting from Ru−N−O bending. Eclipsed on the left, staggered on the right.

Table 3. Electrochemical Data[a] of Complexes

	E_{ox1}	E_{red1}	E_{red2}	E_{red3}
$[Ru(NO_2)(bpym)(terpy)](PF_6)$	0.79[b]	−1.55	−1.93	n.o.
$[Ru(NO)(bpym)(terpy)](PF_6)_3$	n.o.	+0.17	−0.47	−1.61[c]

[a] From cyclic voltammetry at 200 mV/s. Half-wave potentials E in V versus $Fc^{+/0}$ in CH_3CN/0.1 M Bu_4NPF_6. n.o. = not observed. [b] Reversible at 2 V/s at 298 K or at 200 mV/s at −40 °C. [c] Adsorption.

Table 4. UV−Vis Spectroelectrochemical Response for the Conversion $[Ru(NO)(bpym)(terpy)]^{(3+)\rightarrow(2+)\rightarrow(+)}$ in CH_3CN/0.1 M n-Bu_4NPF_6

compounds	λ/nm (ϵ/M^{-1} cm^{-1})
$[Ru(NO)(bpym)(terpy)]^{3+}$	265 (10 800), 291 (8930), 312sh, 331sh, 362 (5120)
$[Ru(NO)(bpym)(terpy)]^{2+}$	268 (11 400), 309 (11 200), 450sh
$[Ru(NO)(bpym)(terpy)]^{+}$	268 (12 440), 306 (12 550), 454 (4500), 743 (680)

dine of terpy and the bpym plane), as depicted in Figure 6. The barrier between two different conformations allows for the detection of two different isomers of [Ru(NO)(bpym)(terpy)]$^{2+}$ with different g factor components at 4 K. ADF/BP calculations give two slightly different sets of g values, viz., $g_1 = 2.0319$, $g_2 = 1.9884$, $g_3 = 1.8907$ and $g_1 = 2.0163$, $g_2 = 2.0000$, and $g_3 = 1.9065$, for the staggered and eclipsed configurations, respectively. These values reproduce the results from the EPR experiments well.

UV−Vis-NIR Spectroelectrochemistry. In comparison to intense metal-to-ligand charge transfer (MLCT) bands involving large π systems such as bpym or terpy, the MLCT absorptions involving NO^+ are usually weak.[8,33] The unreduced [Ru(NO)(bpym)(terpy)]$^{3+}$ thus shows long wavelength absorption maxima at 362 and 312 nm, that is, in the UV region, which most likely comprise d(Ru) → π*(bpym)[27] and d(Ru) → π*(terpy) transitions (Table 4, Figure 7).

Upon one-electron reduction in CH_3CN/0.1 M Bu_4NPF_6, there is additional absorption intensity in the visible region and below 350 nm; however, the first observable band maximum lies at 309 nm. Apparently, transitions involving the half-occupied π*(NO) orbital are too weak to make themselves observable as intense absorption bands. After second reduction, on the other hand, there are two bands in the visible region with maxima at 743 and 454 nm (Table 4, Figure 8). Following the DFT calculations, these low-energy features are attributed to ligand-to-ligand charge transfer (LLCT) transitions from the filled π* MOs of the doubly

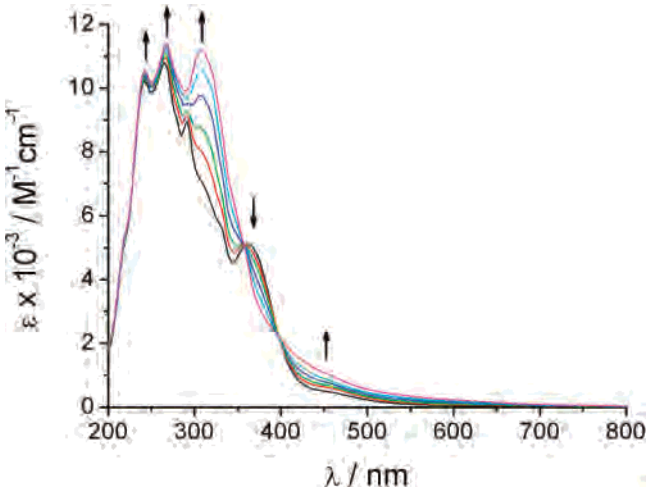

Figure 7. UV−vis spectroelectrochemical response of the conversion [Ru(NO)(bpym)(terpy)]$^{(3+)\rightarrow(2+)}$ in CH_3CN/0.1 M Bu_4NPF_6 at 298 K.

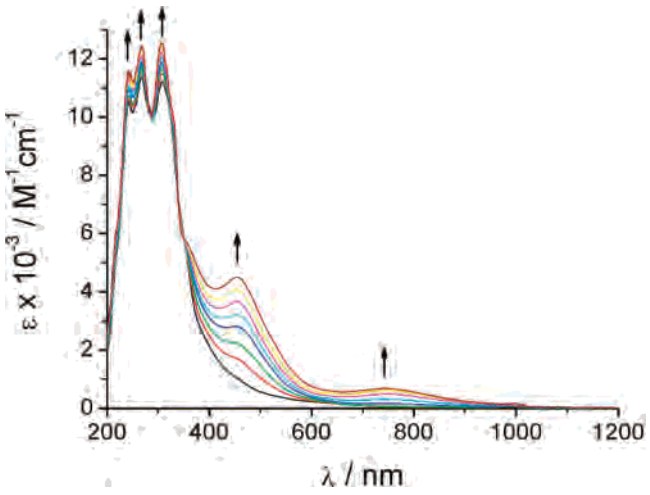

Figure 8. UV−vis spectroelectrochemical response of the conversion [Ru(NO)(bpym)(terpy)]$^{(2+)\rightarrow(+)}$ in CH_3CN/0.1 M Bu_4NPF_6 at 298 K.

Table 5. Selected ADF/BP Calculated Bond Lengths (Angstroms) and Angles (Degrees) for Complexes $[Ru(NO)(bpym)(terpy)]^{n+}$

	$n = 3$	$n = 2$ staggered	$n = 2$ eclipsed
Ru−N1	1.775	1.836	1.891
Ru−N2	2.012	1.988	1.999
Ru−N3	2.121	2.120	2.109
Ru−N4	2.121	2.116	2.114
Ru−N5	2.126	2.119	2.111
Ru−N6	2.136	2.120	2.139
N1−O1	1.143	1.185	1.188
O−N1−Ru	177.4	147.3	139.6

reduced nitrosyl ligand, that is, electron rich NO^-,[8a] to the higher-lying, still-empty π* orbitals of the bpym and terpy acceptors. The interpretation of a π* MO energy sequence (NO) < bpym < terpy is supported by the above results and by the less-negative reduction potential of free bpym (−1.73 V vs SCE)[27,34a] versus free terpy (−2.00 V vs SCE)[26,34b] as well as by DFT calculations.

DFT Calculations. As documented in Table 2, the DFT optimized geometries describe the experimental structure of

(33) Paulat, F.; Kuschel, T.; Näther, C.; Praneeth, V. K. K.; Sander, O.; Lehnert, N. *Inorg. Chem.* **2004**, *43*, 6979.

(34) (a) Ernst, S.; Kaim, W. *J. Am. Chem. Soc.* **1986**, *108*, 3578. (b) Saji, T.; Aoyagui, S. *Electroanal. Chem. Interfac. Electrochem.* **1975**, *58*, 401.

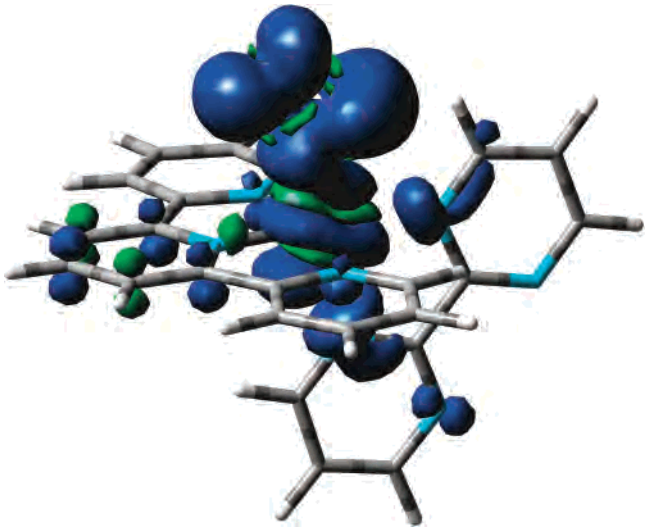

Figure 9. Representation of spin density in the eclipsed conformation of $[Ru(NO)(bpym)(terpy)]^{2+}$.

unreduced $[Ru(NO)(bpym)(terpy)]^{3+}$ well. The added electron causes the largest changes in the Ru−N−O part of the molecule, characterized by a Ru−N−O angle bending to about 140−147° and elongation of the Ru−N and N−O bonds, depending on the conformation. Table 5 shows the variation of ADF/BP calculated bond parameters, the analogous geometry variations due to the reduction were obtained by G03/B3LYP calculations.

The geometry variation in the course of the reduction reflects the electronic structure of $[Ru(NO)(bpym)(terpy)]^{3+}$. In this complex, the lowest unoccupied molecular orbital (LUMO) is of *e* symmetry, on the basis of the π^* orbitals of the nitrosyl ligand (around 66%) with 23% contributions from 4d orbitals of ruthenium and 10% from π^* orbitals of the bpym and terpy ligands. Closely lying occupied and unoccupied molecular orbitals are mainly formed by the π orbitals of the bpym and terpy ligands, with small contributions from metal d orbitals (less than 10%). During the reduction, the added electron is accepted by the LUMO, and the originally degenerate *e* orbital splits into nondegenerate ones. Figure 9 shows the distribution of spin density in $[Ru(NO)(bpym)(terpy)]^{2+}$ resulting from the single occupancy of an NO-based redox orbital.

The G03/BPW91 calculations slightly underestimate the ν(NO) stretching frequency (calculated at 1939 cm^{-1}); however, the uptake of an electron into the NO-based LUMO is indeed reflected by the lowering of this band by 216 cm^{-1}. The second reduction causes a further low-energy shift of 181 cm^{-1}. Scaled B3LYP values indicate shifts of similar size. The underestimation of frequency shifts is probably caused by the overestimation of the Ru 4d contribution to the redox orbital.

Conclusions

The combination of three different π-acceptor ligands bonded to ruthenium(II) in $[Ru(NO)(bpym)(terpy)](PF_6)_3$ has resulted in the opportunity to study two one-electron reduction processes, both of which involve the NO ligand. The

Scheme 1

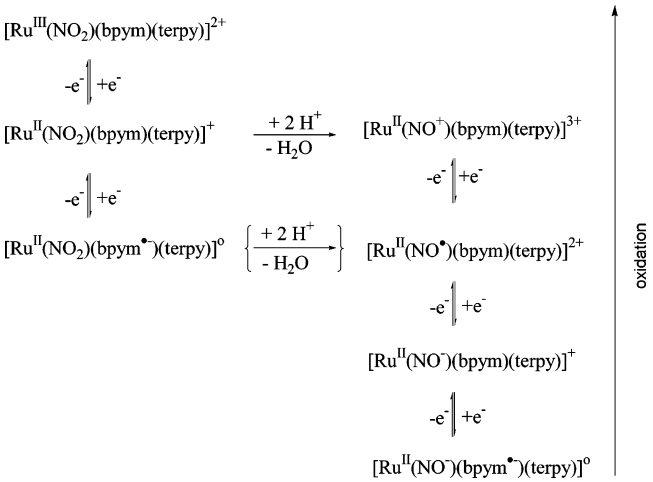

stability of the paramagnetic intermediate $[Ru(NO)(bpym)(terpy)]^{2+}$ could be used to study the EPR behavior by high-frequency methods, which revealed the existence of two species, probably conformers. Whereas the UV−vis spectra of this intermediate are inconspicuous, the doubly reduced form $[Ru(NO)(bpym)(terpy)]^{+}$ exhibits absorption bands in the visible region, which are attributed to LLCT transitions. Taken together with the more conventional response from the nitro precursor complex, Scheme 1 illustrates how the conversion from the NO_2^- to the NO^n ligand does not only shift the reduction potentials but also results in a completely different electron-transfer series by the insertion of a π^*-(NO) orbital as the lowest unoccupied MO.

Accordingly, one of the perspectives arising from this work involves the NO_2^-/NO^+ conversion[35] of the one-electron reduced forms in comparison to the nonreduced species; dinuclear bpym-bridged compounds are also of interest because of the possibility to study the ligand-mediated interaction of complex entities $\{RuNO\}^n$ instead of metal centers with only innocent ancillary ligands.[36]

Acknowledgment. This work was supported by the Deutsche Forschungsgemeinschaft (DFG), the Fonds der Chemischen Industrie (FCI), the European Union (COST D35), the Grant Agency of the Academy of Sciences of the Czech Republic (KAN100400702), and Ministry of Education of the Czech Republic (OC 139).

Supporting Information Available: X-ray crystallographic files in CIF format with molecular structure figures for $[Ru(NO_2)(bpym)(terpy)](PF_6)$, $[Ru(NO)(bpym)(terpy)](PF_6)_3$, and $[Ru(CH_3CN)(bpym)(terpy)](PF_6)_3$; EPR spectra of $[Ru(NO)(bpym)(terpy)]^{2+}$ at X band (9.5 GHz) and W band (95 GHz) frequencies. This material is available free of charge via the Internet at http://pubs.acs.org.

IC701206A

(35) (a) Olabe, J. A. *Adv. Inorg. Chem.* **2004**, *55*, 61. (b) Roncaroli, F.; Videla, M.; Slep, L. D.; Olabe, J. A. *Coord. Chem. Rev.* **2007**, *251*, 1903.

(36) (a) Sarkar, B.; Kaim, W.; Fiedler, J.; Duboc, C. *J. Am. Chem. Soc.* **2004**, *126*, 14706. (b) Kaim, W.; Lahiri, G. K. *Angew. Chem.* **2007**, *119*, 1808; *Angew. Chem., Int. Ed.* **2007**, *46*, 1778.